The suppressive effect of TGFβ-1 on EIU may be speculated further by its interaction with inducible nitric oxide synthase (iNOS). TGFβ-1 reduces iNOS mRNA translation and increases degradation of iNOS protein in macrophages. Inhibition of EIU has been achieved by inhibition of NOS.[10]

In summary, the current study has demonstrated that systemic TGFβ-1 is able to suppress acute uveitis in the mouse. The mechanism involves the TGFβ-1 effect on multiple cytokines and inflammatory mediators that are produced during the course of EIU. TGFβ-1 may become a potential therapeutic cytokine for patients with uveitis.

Key Words

cytokine, endotoxin-induced uveitis (EIU), interleukin-6, ocular inflammation, transforming growth factor beta-1 (TGFβ-1)

References

1. Roberts AB, Sporn MB. Transforming growth factor β. *Adv Cancer Res.* 1988;51:107–144.
2. Walh SM. Transforming growth factor beta (TGF-β) in inflammation: A cause and a cure. *J Clin Immunol.* 1992;12:61–74.
3. Kuruvilla AP, Shah R, Hochwald GM, Liggitt HD, Palladino MA, Thorbecke GJ. Protective effect of transforming growth factor β-1 on experimental autoimmune diseases in mice. *Proc Natl Acad Sci USA.* 1991;88:2918–2921.
4. Li Q, Sun B, Dastgheib K, Chan CC. Suppressive effect of transforming growth factor β1 on the recurrence of experimental melanin-protein induced uveitis: Upregulation of ocular interleukin-10. *Clin Immunol Immunopathol.* 1996;81:55–61.
5. Li Q, Peng B, Whittcup SM, Jang SU, Chan CC. Endotoxin induced uveitis in the mouse: Susceptibility and genetic control. *Exp Eye Res.* 1995;61:629–632.
6. de Vos AF, van Haren MA, Verhagen C, Hoekzema R, Kijlstra A. Kinetics of intraocular tumor necrosis factor and interleukin-6 in endotoxin-induced uveitis in the rat. *Invest Ophthalmol Vis Sci.* 1994;35:1100–1106.
7. Planck SR, Huang XN, Robertson JE, Rosenbaum JT. Cytokine mRNA levels in rat ocular tissues after systemic endotoxin treatment. *Invest Ophthalmol Vis Sci.* 1994;35:924–930.
8. Peng B, Li Q, Roberge FG, Nussenblatt RB, Chan CC. The role of transforming growth factor β1 (TGFβ1) in endotoxin induced uveitis (EIU). ARVO Abstracts. *Invest Ophthalmol Vis Sci.* 1995;36:S545.
9. Benveniste EN, Tang LP, Law RM. Differential regulation of astrocyte TNF-alpha expression by the cytokines TGF-beta, IL-6 and IL-10. *Int J Dev Neurosci.* 1995;13:341–349.
10. Parks DJ, Cheung MK, Chan CC, Roberge FG. The role of nitric oxide in uveitis. *Arch Ophthalmol.* 1994;112:544–546.

Modeling Spatial Integration and Contrast Invariance in Visual Pattern Discrimination

Risto E. Näsänen, Heljä T. Kukkonen, and Jyrki M. Rovamo

Purpose. Human pattern discrimination performance has been reported to be largely independent of stimulus contrast but to depend on stimulus area. The authors propose a model that combines the effects of spatial integration and contrast. The model is based on the computation of similarity between pattern templates in memory and signals to be discriminated using normalized correlation. There are also two sources of additive noise, one before and one after the computation of correlation. The model was compared with human observers in an orientation discrimination task.

Methods. Orientation discrimination thresholds of human observers were measured for sinusoidal gratings of various areas, contrasts, and spatial frequencies. A two-interval, forced-choice method was used. The performance of the model was determined by using computer simulations.

Results. It was found that the effects of contrast and grating area were interrelated: The decrease of orientation thresholds as a function of grating area was considerably larger at low than at high contrast. On the other hand, orientation thresholds decreased clearly as a function of contrast at the smallest grating areas but hardly at all at the largest grating areas. The model accounted well for the experimental findings.

Conclusions. Because the invariance of orientation discrimination with respect to stimulus contrast depended on area, the cause of the invariance appeared to occur after spatial integration. The model explains this so that, with increasing contrast or area, the normalized correlation gradually approached a constant value. The proportion of pretemplate noise became negligible compared to the constant posttemplate noise. Thus,

From the Department of Optometry and Vision Sciences, University of Wales, College of Cardiff, Cardiff, United Kingdom.
Received for publication March 7, 1996; revised September 3, 1996; accepted September 5, 1996.
Proprietary interest category: N.
Reprint requests: Risto E. Näsänen, Department of Optometry and Vision Sciences, University of Wales, College of Cardiff, Redwood Building, King Edward VII Avenue, Corbett Road, Cardiff CF1 3XF, United Kingdom.

total noise also approached a constant value. Hence, the signal-to-noise ratio and discrimination performance became constant. Invest Ophthalmol Vis Sci. 1997;38:260–266.

Thresholds for discriminating pattern features, such as spatial frequency and orientation, have been found to decrease with contrast only at low-contrast levels. At higher contrasts, thresholds become independent of contrast.[1–3] The constancy of pattern discrimination thresholds as a function of contrast suggests that the signal-to-noise ratio at the decision stage is independent of contrast. Various explanations, including multiplicative noise, logarithmic response of pattern-sensitive mechanisms,[2] and "computation" of signal attributes (such as spatial frequency, orientation, and contrast, each followed by additive "task-dependent" noise[3]) have been considered.

In external spatial noise, orientation thresholds have been found to decrease considerably with increasing grating area.[4] Spatial integration is, however, smaller for human observers than for the ideal observer, which compares the input signal with previously learned pattern templates in memory. Discrimination efficiencies are high for gratings of small numbers of square cycles, but they decrease rapidly as a function of area. These results can be explained by assuming that spatial integration is performed by an ideal discriminator operating only within a spatial integration window, whose size is scaled according to the resolution at which the image is inspected. The idea of a window has been suggested in articles concerning human pattern recognition[5] and contrast detection.[6]

In this report, we model spatial integration and contrast invariance of orientation discrimination of simple sinusoidal gratings. The limitation of spatial integration was obtained by using templates with a window-weighting function.[4] To account for the contrast constancy, we used a contrast-independent measure, normalized correlation, to compute the similarity (template matching) of signal presented and pattern templates in memory. The performance of the model was compared with experimental results obtained with human observers. Human orientation discrimination thresholds were measured as a function of grating contrast, area, and the range of contrast randomization.

The Model. In white gaussian noise, the ideal discriminator and the pattern recognition observer compares the input signal with a set of templates by computing the Euclidean distance between the signal and each template.[7,8] To identify the signal, the observer looks for the template with the shortest distance to the signal. The Euclidean distance (D_i) between noisy signal $s_n(x,y)$ and template $m_i(x,y)$ is computed as

$$D_i = \left\{ \sum_x \sum_y [s_n(x,y) - m_i(x,y)]^2 \right\}^{1/2}. \quad (1)$$

For noisy signals, distance D_i varies from trial to trial. This limits the minimum discernible difference (threshold) between the patterns to be identified.

The Euclidean distance is not, however, insensitive to variations in signal and template contrasts. A highly efficient but contrast invariant method to compute the similarity between a template and an input signal is the normalized correlation R_i, which can have values only between −1 and +1. Normalized correlation (or the correlation coefficient) is defined as

$$R_i = \iint s_n(x,y)\, m_i(x,y)\, dx\, dy \Big/ \left[\iint s_n(x,y)^2 dx dy \iint m_i(x,y)^2 dx dy \right]^{1/2}. \quad (2)$$

After the normalized correlations of signal $s_n(x,y)$ with each $m_i(x,y)$ have been computed, the identification of the signal is based on the largest R_i found. Our computer simulations showed that, in simple orientation discrimination, normalized correlation is as good as the Euclidean distance. Because of its contrast invariance, we chose to use the normalized correlation as the discriminator in our model.

It is well known that spatial integration in human vision is limited. As in our previous article,[4] the limitation of spatial integration was modeled using a window function

$$w(r) = \frac{1}{(1 + (rf/r_o)^3)}, \quad (3)$$

where $r = \sqrt{(x^2 + y^2)}$ is the distance from the window center, r_o is the distance in cycles at which $w(r) = {}^1/_2$, and f is the spatial frequency of the grating. The model was fitted to the current data (Figs. 1 to 3) with $r_o = 1$ and 0.75 for observers REN and HTK, respectively. The template $m_i(x,y)$ for a signal is the product of the window function and internal signal $s'_i(x,y)$. The prime is to denote that external signal $s_i(x,y)$ is filtered[9] by a low-pass transfer function (primarily because of the optics of the eye) and by a composite neural high-pass transfer function, which represents the combined effect of possibly many stages of neural processing.

$$m_i(x,y) = w(r)\, s'_i(x,y). \quad (4)$$

Because in this report the model is applied only

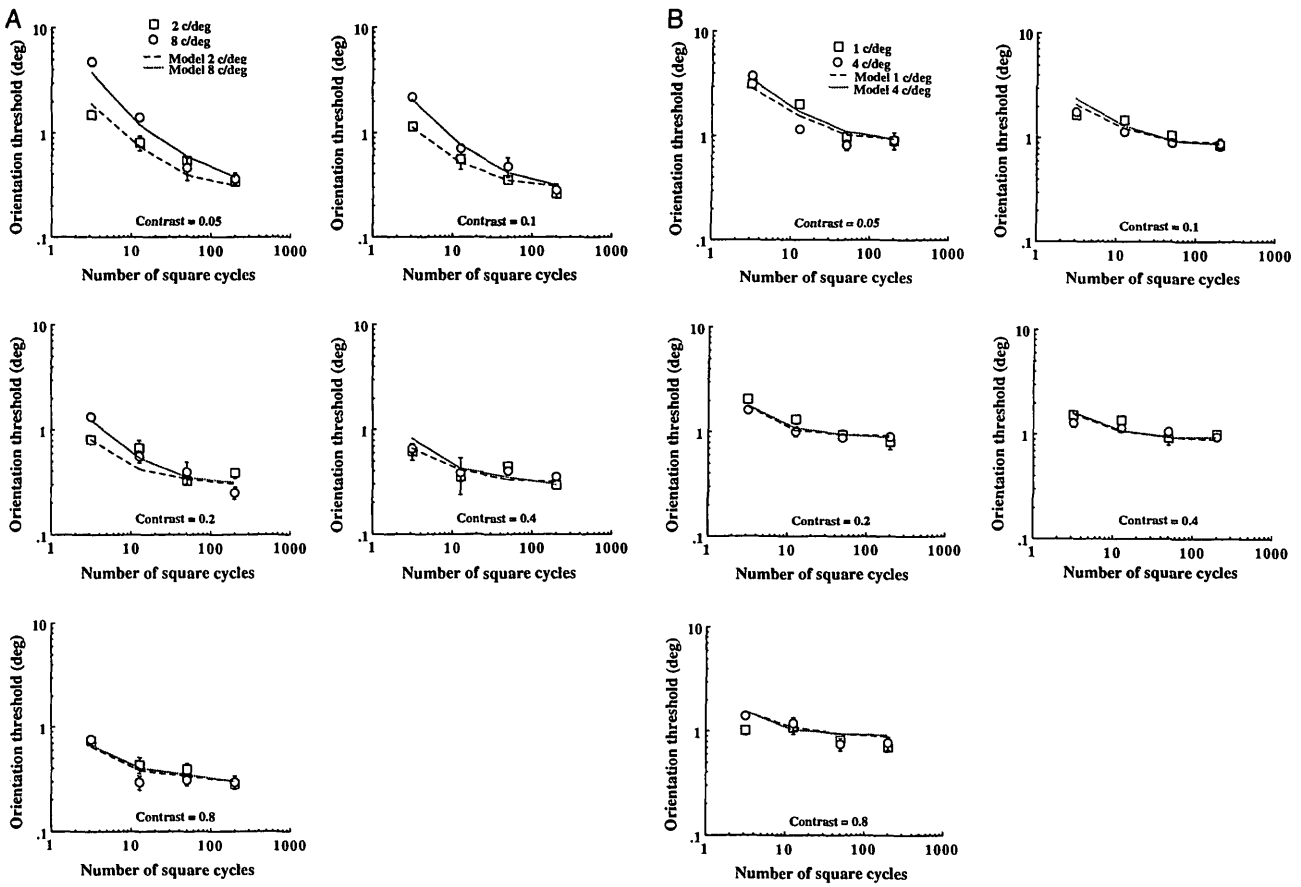

FIGURE 1. Orientation discrimination thresholds for sinusoidal gratings as a function of the number of square cycles at different contrast levels for observers REN (**A**) and HTK (**B**). The error bars show ± 1 standard error of the mean. Where there are no error bars, the standard error is smaller than the symbol size. Dashed and dotted lines show the performance of the model.

to grating stimuli of relatively small spatial bandwidth, we approximate the filtering by multiplying the contrast of the external signal by the transfer functions:

$$s'(x,y) \approx H_o(f)H_n(f)s(x,y), \quad (5)$$

where f is the spatial frequency of the grating.

The low-pass transfer function used[9] is

$$H_o(f) = \frac{1}{(1 + (f/7.2)^3)}. \quad (6)$$

The neural high-pass transfer function[9] is

$$H_n(f) = f. \quad (7)$$

It is assumed that there are two sources of neural noise, one before and one after the computation of the normalized correlation. Neural noise is spatiotemporal. However, for simplicity, we describe neural noise by its spatial equivalent, which has an effect equal to that of internal spatiotemporal noise. The signal with neural noise is

$$s_n(x,y) = s'(x,y) + n(x,y), \quad (8)$$

where $n(x,y)$ is a noise waveform with a given spectral density N_i. Spectral density describes the variance of noise per unit spatial frequency. The noise in the simulation was white, that is, its spectral density N_i is constant across spatial frequencies. Spectral density of pixel noise can be computed as the product of the noise root-mean-square-contrast squared and pixel area.[10]

The decision variable Q_i is the sum of normalized correlation R_i from equation 2 and posttemplate noise ρ:

$$Q_i = R_i + \rho. \quad (9)$$

In equation 9, posttemplate noise ρ is a gaussian random variable with a given standard deviation (σ_ρ).

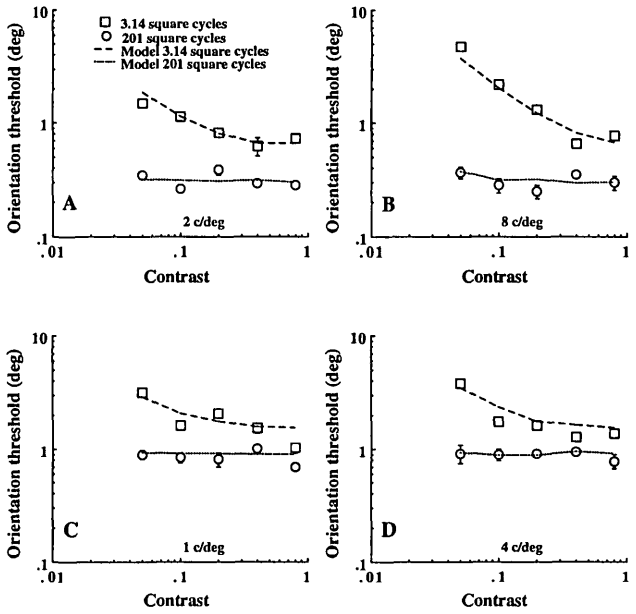

FIGURE 2. Orientation discrimination thresholds for 2 and 201 square cycle gratings as a function of contrast for observers REN (**A,B**) and HTK (**C,D**). Dashed lines show the performance of the model.

The model observer identifies the input signal by searching for the template for which Q_i is largest. The random variation of R_i caused by pretemplate noise together with posttemplate noise ρ limits the smallest distance between the signals to be discriminated.

The pretemplate noise has two effects. First, it reduces the average value of R_i; second, it produces variance. At very low signal contrasts, R_i increases with increasing contrast, but the increase saturates at higher contrasts. At the same time, the variance caused by pretemplate noise decreases. Therefore, posttemplate noise, which is independent of contrast, becomes the dominant source of noise. Because at high contrast each R_i and the standard deviation of noise are independent of contrast, the signal-to-noise ratio remains constant. The free parameters of the model and their values for observers REN and HTK are listed in Table 1.

In the computation of the normalized correlation, there are two normalizing factors, the energies of the signal ($s_n(x,y)$) and the template ($m_i(x,y)$). Template energy is limited by the window function, but because the signal is not windowed, signal energy reduces the normalized correlation if the signal is very large (diameter $>$ ~30 cycles). Consequently, orientation thresholds would increase. Therefore, we assume that the integration does not extend more than 30 cycles. In the experiments in this study, the largest grating diameter measured only 16 cycles.

In the experiments, observers were given feedback about the correctness of responses. This made it possible to update continuously the memory templates when the difference of grating orientations became smaller. The learning process itself was not modeled here, and it was assumed that the template updating by human observers was highly accurate. In the experiments the signal phase was randomized. Because the signals were always well above the detection threshold, we assumed that human observers were capable of locating the template to the optimal position with respect to the signal phase. Therefore, we did not model the search for the optimum location.

Orientation discrimination thresholds of the model were determined using computer simulations. The threshold orientation difference between the two grating stimuli was searched for iteratively so that at threshold the probability of correct responses was 0.84, the same value used in the experiments with human observers.

METHODS. Stimuli were generated using a 486 personal computer and an Eizo Flexscan 9080i monitor (Eizo Corp., Japan). Resolution of the graphics was 640 × 480 pixels. Pixel size was 0.42 × 0.42 mm^2. Average photopic luminance of the display was 50 cd/m^2. Nonlinearity of the luminance response of the display was corrected by using the inverse function of the luminance response when the stimuli were computed.

The stimuli were sinusoidal gratings of 2 cyc/cm within a circular aperture. The diameter of the aperture was 1, 2, 4, or 8 cm. The phase of the gratings was randomized between 0° − 360° in each stimulus presentation.

Stimuli were viewed binocularly at the distances of 28.5, 57, 114, and 229 cm with natural pupils 5 to 6 mm in diameter. Spatial frequencies varied between 1 and 8 cyc/deg. Duration of stimulus exposures was 500 msec. The two exposures of each trial were separated by 600 msec, and a new trial began 250 msec after the observer's response.

Thresholds were determined using a two-interval forced-choice algorithm. One of the two successive exposures contained a vertical grating, and the other contained a grating rotated counterclockwise. Observers indicated whether the rotated grating was shown during the first or second exposure by pressing one of two keys on the computer keyboard.

After four consecutive correct responses, the orientation difference between the tilted and vertical gratings was decreased by a multiplicative factor of 1.26; after each incorrect response, the difference was increased by the same factor. Auditory feedback was given for an incorrect response. A threshold estimate at the probability level of 0.84 was obtained as the mean of eight reversals. Each data point shown in Figure 2 represents the mean of three to six threshold estimates.

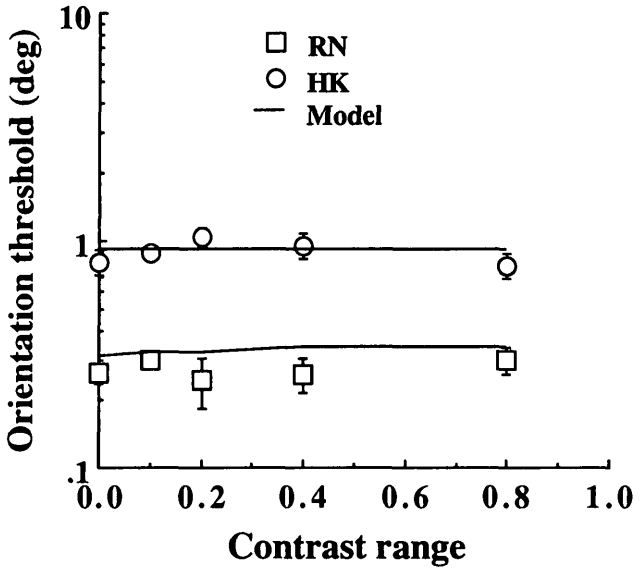

FIGURE 3. Orientation discrimination thresholds as a function of the range of contrast randomization. Mean Michelson contrast was 0.5. Contrasts in the two intervals were randomized independently of each other. Solid lines show the performance of the model.

Two subjects, one with corrected myopia (−4.25 D) (REN) and one with uncorrected hyperopia (+0.5 D) (HTK), served as observers. REN has a visual acuity of 2.0, and HTK's visual acuity is 1.3. Visual acuities were measured with an Oriola test chart (Oriola, Espoo, Finland) based on Sloan letters. Tenets of the Declaration of Helsinki were followed, informed consent was obtained, and institutional human experimentation committee approval was granted before the experiments were conducted.

RESULTS. In the first experiment, we measured orientation discrimination thresholds as a function of grating area at different contrasts. Results for subjects REN and HTK are shown in Figure 1 and were plotted as a function of the number of square cycles, obtained as the product of grating area and spatial frequency squared. At low contrast, there was a substantial decrease in orientation discrimination thresholds when the number of square cycles increased. Thus, there was clear spatial integration. With increasing contrast, the curves became shallower, and spatial integration became weaker.

The change of spatial frequency was produced by changing the viewing distance. Thus, at each value of square cycles, different spatial frequencies represented different magnifications of the same stimuli. For each subject, the orientation thresholds measured at the two spatial frequencies (2 and 8 cyc/deg, REN, Fig. 1A; 1 and 4 cyc/deg, HTK, Fig. 1B) were nearly similar. The only exceptions were the low-contrast results for the 8 cyc/deg grating (contrast was attenuated by the optics of the eye). Therefore, it seems that orientation discrimination is scale invariant as long as the attenuating effect of the optics of the eye is not too large.

In Figure 2, the results for gratings of 2 and 201 square cycles were plotted as a function of contrast. As Figure 2 shows, there was a decline in thresholds for 2 square cycles, whereas the orientation thresholds for 201 square cycles were nearly constant.

Results shown in Figures 1 and 2 show that the effects of contrast and area on orientation discrimination depend on each other. Solid and dotted lines in Figures 1 and 2 represent the fit of the model to the data. The model accounts well for all the experimental results. To estimate the goodness of fit, we computed the average (root-mean-square) relative error (ϵ) between the fit of the model (m_i) and experimentally measured values (s_i) using the following equation:

$$\epsilon = \sqrt{\{[\sum_{i=1}^{n} (m_i - s_i)^2/s_i^2]/n\}}. \quad (10)$$

The average relative errors were 19% and 16% for observers REN and HTK, respectively.

To demonstrate the solidity of contrast invariance, we conducted an additional experiment in which orientation discrimination thresholds were measured as a function of the range of contrast randomization. The randomization of the contrasts of the two intervals were independent of each other. Random contrast values were samples of an even distribution. The mean Michelson contrast was 0.5, and the contrast randomization ranges were 0, 0.1, 0.2, 0.4, and 0.8. The size of the grating was 50 square cycles, and the spatial frequency was 4 cyc/deg. Results for the two observers are shown in Figure 3. They show that contrast ran-

TABLE 1. Free Parameters of the Model

Parameter	*Meaning*	*REN*	*HTK*
r_o	Width parameter of window	1	0.75
N_i	Spectral density of internal noise (deg^2)	15×10^{-6}	10×10^{-6}
σ_p	Standard deviation of posttemplate noise	0.5×10^{-3}	2.5×10^{-3}

REN = values for observer REN; HTK = values for observer HTK.

domization had hardly any effect on orientation thresholds. The continuous line shows the fit of the model to the experimental data.

DISCUSSION. Results showed that orientation discrimination thresholds decreased with grating area. At higher contrasts, the effect of area became small. In agreement with previous studies,[1,2] orientation discrimination thresholds were independent of contrast. This, however, applied only to large grating areas. At small grating areas, orientation discrimination thresholds decreased with contrast.

The fact that the effect of contrast depends on area suggests that the factors that cause the constancy of orientation discrimination threshold with increasing grating contrast occur after spatial integration. Orientation discrimination performance depended on the number of square cycles rather than on the absolute grating area in degrees squared. Orientation discrimination was, therefore, scale invariant so that magnification or minification of the stimulus did not affect thresholds at low and medium spatial frequencies, where there is little attenuation because of the optics of the eye. At the highest spatial frequency used (8 cyc/deg), deviations from the complete scale invariance were well explained by the model, which took the effects of optics into account.

The model successfully explained all the experimental findings and was based on normalized correlation computed between the input signal and two templates, one for each alternative. There were two sources of noise, one before and one after the computation of normalized correlation. With increasing contrast or grating area, the effect of pretemplate noise decreased. As a result, the normalized correlation increased, approaching a constant. Meanwhile, the posttemplate noise remained constant. Therefore, the signal-to-noise ratio, as well as discrimination performance, approached constant values.

Contrast invariance in pattern discrimination has been modeled in different ways. Thomas[11] suggested that the responses of the mechanisms sensitive to each stimulus alternative are followed by noise whose standard deviation increases in direct proportion to the increase of responses. Hence, the signal-to-noise ratio remains constant.

Smith and Thomas[2] provided another possible explanation. This one states that there is logarithmic nonlinearity after the responses of the mechanisms sensitive to the stimulus alternatives. This is followed by signal independent noise with constant standard deviation (σ). Because at different contrast levels the ratio of the original responses (R_1/R_2) is constant, the difference of the logarithmic responses ($d = \log(R_1) - \log(R_2) = \log(R_1/R_2)$) is also constant. Thus, the signal-to-noise ratio (d/σ) is independent of contrast. The results of Smith and Thomas[2] support the logarithmic responses rather than the increasing noise model.

Both these principles can be applied to the model described in this report. First, we can remove the normalization in the computation of correlation. Then we can either make the magnitude of the posttemplate noise directly proportional to the unnormalized correlations or take the logarithm of the unnormalized correlations and leave the posttemplate noise constant. Qualitatively, both methods work in the same way as the normalized correlation suggested in this report. On the basis of the current data, it is not possible to rule out any of these alternatives.

Bowne[3] suggested a model in which stimulus properties such as orientation, spatial frequency, and contrast are computed separately and in which each computation is followed by independent additive central noise. Because the computation of orientation or spatial frequency is independent of contrast, the thresholds do not vary with contrast (actually, Bowne did not specify how the computations of the stimulus parameters would be carried out). In Bowne's model, there was also peripheral noise before the computation of stimulus parameters. Bowne's "peripheral" and "central" noises can be regarded to correspond to our pretemplate and posttemplate noises. On the other hand, the computation of the normalized correlation is independent of contrast, such as Bowne's computation of stimulus parameters.

Bowne's suggestion that contrast and stimulus spatial (and temporal) properties are handled separately is supported by the well-known fact that the contrast dependence of contrast discrimination and other discriminations are different. Although spatial and temporal discriminations are largely independent of contrast, contrast discrimination threshold increases as a power function of pedestal contrast with an exponent smaller than unity.[12] The increasing noise model[11] and the logarithmic responses model[2] would predict that contrast discrimination thresholds increase linearly with contrast. Our model would not discriminate contrasts at all at high contrast levels because the normalized correlations are independent of contrast. Therefore, contrast may be a stimulus dimension analyzed independently of spatial shape.

Spatial integration properties of the model are determined by the window-weighting function. Although the orientation discrimination threshold curves are shallower for high-contrast than for low-contrast gratings, the same window-weighting function explains discrimination results at all contrast. The current analysis suggests that the extent of the spatial integration of signal information is independent of contrast.

As Näsänen et al[4] have shown, the same window

function can explain spatial integration in orientation discrimination and contrast discrimination. The window function also accounts for the spatial integration in contrast detection.[13] This suggests that the window function is independent of the nature of the task but that it depends only on the properties of the signal.

The primary purpose of this report was to investigate and to model spatial integration in suprathreshold vision. The intended scope of the current model is limited to the contrast and area dependence of orientation discrimination. How well the model accounts for performance in other discrimination tasks and with complex stimuli will have to be tested by further experiments.

Key Words

ideal observer, noise, orientation, pattern discrimination, spatial integration

References

1. Regan D, Beverley KI. Postadaptation orientation discrimination. *J Opt Soc Am A.* 1985;2:147–155.
2. Smith BG, Thomas JP. Why are some spatial discriminations independent of contrast. *J Opt Soc Am A.* 1989;6:713–724.
3. Bowne SF. Contrast discrimination cannot explain spatial frequency, orientation or temporal frequency discrimination. *Vision Res.* 1990;30:449–461.
4. Näsänen RE, Kukkonen HT, Rovamo JM. A window model for spatial integration in human pattern discrimination. *Invest Ophthalmol Vis Sci.* 1995;36:1855–1862.
5. Nakayama K. The iconic bottleneck and the tenuous link between early visual processing and perception. In: Blakemore C, ed. *Vision: Coding and efficiency.* New York: Cambridge University Press; 1990:411–422.
6. Burgess AE. High level of visual decision efficiencies. In: Blakemore C, ed. *Vision: Coding and Efficiency.* New York: Cambridge University Press; 1990:431–440.
7. Duda RO, Hart PE, *Pattern Classification and Scene Analysis.* New York: John Wiley & Sons; 1973.
8. Tjan BS, Braje WL, Legge GE, Kersten D. Human efficiency for recognizing 3-D objects in luminance noise. *Vision Res.* 1995;21:3053–3069.
9. Rovamo J, Luntinen O, Näsänen R. Modelling the dependence of contrast sensitivity on grating area and spatial frequency. *Vision Res.* 1993;33:2773–2788.
10. Legge GE, Kersten D, Burgess AE. Contrast discrimination in noise. *J Opt Soc Am A.* 1987;4:391–404.
11. Thomas JP. Underlying psychometric function for detecting gratings and identifying spatial frequency. *J Opt Soc Am.* 1983;73:751–758.
12. Legge GE, Foley JM. Contrast masking in human vision. *J Opt Soc Am.* 1980;70:1458–1471.
13. Näsänen R, Syväjärvi A, Rovamo J. Effect of image orientation contents on detection efficiency. *Vision Res.*, In press.